

# Investigation of the effect of porosity on the particle deposition efficiency in the model of an open cell foam filter

O V Soloveva, R R Khusainov, E G Sheshukov and R R Yafizov

Institute of Heat Power Engineering, Kazan State Power Engineering University,  
Krasnoselskaya st. 51, Kazan, 420066, Russian Federation

E-mail: solovyeva.ov@kgeu.ru

**Abstract.** In this work, we performed experimental and numerical simulation of gas flow in the model of the open cell foam filter. We investigated the relationship between the porosity of the medium  $\varepsilon$ , and the parameter  $Po$  characterizing the number of pores per inch. We obtain a porous medium from the inverse matrix of the computational model made on a 3D printer. The calculation results of the pressure drop depending on the average filtration rate correlate well with the experimental data. Particle trajectories make it possible to determine the particle deposition efficiency in a porous layer for three values of the porosity of the medium  $\varepsilon = 0.6$ ,  $\varepsilon = 0.7$  and  $\varepsilon = 0.8$ . The deposition efficiency in the case of porosity  $\varepsilon = 0.8$  correlate well with the data obtained by the semi-empirical formula of the authors of [1], however, for the other two values of the porous medium, the efficiency curves differ significantly, so the dependence was obtained for a material with high porosity. We define the filter quality parameter by the ratio of the particle deposition efficiency to the pressure drop value in the porous layer.

## 1. Introduction

Open cell foams have a very diverse use [2-10]. They are used as thermal insulation [11, 12], in heat exchange amplifiers in electrical systems, where the radiator is extremely important [13, 14], as receivers of solar radiation [15, 16], and as open cell foam matrix catalyst using instead of industrial catalysts [17]. Also, the open cell foam material is used as an active filter for aerosol particles due to the low drag coefficient and developed surface [18-21].

For the gas flow numerical simulation in the porous medium, it is necessary to make a geometric model that will correspond to the real structure of the material. The authors of [22-24] use a porous medium from simplified cells with an ordered structure. However, the real porous medium structure is not orderly, and it provides significant changes in the flow hydrodynamics. A model that represents the actual structure can be obtained using microtomography technology [15, 16]. The model obtained by the microtomography of the medium further requires long and laborious processing, cleaning from «suspended in space» elements that are not related to the general structure. The disadvantage of this method is that the resulting geometry requires lengthy and time-consuming processing. Modern technologies make it possible to print material on a 3D printer with specified parameters of a porous medium. Due to the complex shape of the porous media geometry, the majority of published works based on experimental data [25, 26].

The use of simplified models of the flow in porous structures leads to significant differences in experimental and calculated data [27-30]. There are experimental studies of heat and mass transfer in a porous medium [16, 23, 25-29].

The authors of the work [31] compare the heat exchanger performance with the open cell foam material and with finned tubes. The results show that the open cell foam material not only intensifies the heat transfer but at the same time reduces the weight and size of the heat exchanger. The work [32] presents the results of heat transfer measuring inside rectangular aluminum blocks, with a constant supply of heat to the porous medium. The authors propose an analytical model for heat exchange in a metallic porous medium. In [33], the authors investigated the effect of the open cell foam material thickness on the heat transfer properties and pressure drop in the vertical channel.

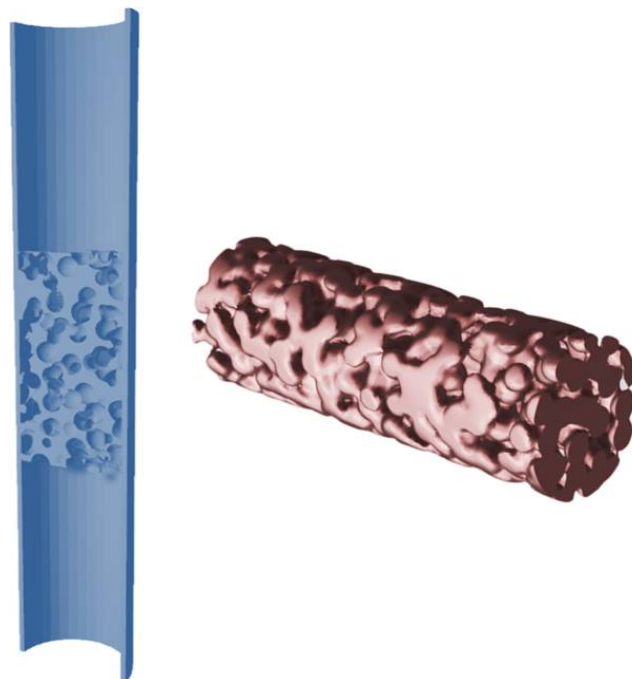
Numerical simulation of processes in porous media can overcome all experimental problems and accurately take into account the smallest geometric details. Modern computational capabilities make it possible to create a detailed geometry of the computational area, set the material properties and boundary conditions.

Previously, researchers based their numerical studies of porous media mainly on the averaged volume method and the Darcy law. In [34], the authors made a detailed numerical simulation of the flow in a metallic open cell foam material. Detailed numerical simulation is the most accurate method for studying flow in porous filters, because it is inapplicable to many averaged flow models in porous media due to a complex porous material structure.

The purpose of this work is to determine the pressure drop value in the open cell foam material, which is a model of an aerosol filter, and the particle efficiency deposition for three values of medium porosity.

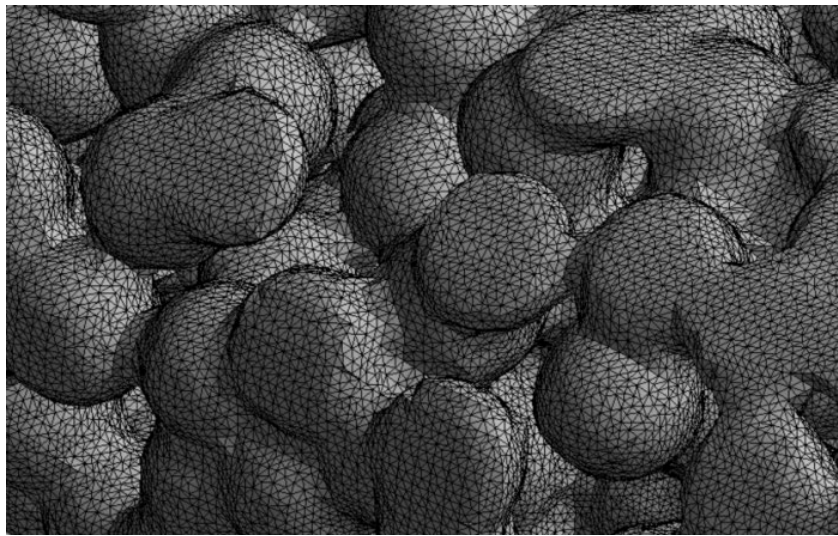
## 2. Problem formulation

Let us make experimental studies and numerical simulation of the air flow in open cell foam material with different medium porosity  $\varepsilon$  (the ratio of the pore volume in the total body volume) and a fixed pore size  $d_c = 4$  mm. The computational model of an open cell foam filter is a set of intersecting spheres randomly arranged in space. (Fig. 1).



**Figure 1.** The porous medium computational model for cells diameter  $d_c = 4$  mm.

We made calculations in the ANSYS Fluent software package (v. 19.0) for the viscous incompressible gas model by solving the Navier-Stokes equations using the finite volume method. There are two main approaches to describe gas flow in a porous medium. The first approach is based on the averaged flow models that include an adjustment for the medium porosity (and permeability), such as, the well-known Darcy model. The second approach involves the calculation of the flow in a porous medium based on the Navier-Stokes equations, taking into account the geometry details. This approach is the most accurate because it takes into account the pores shape, pore location, fiber diameter, and other parameters. In this case, taking into account the resistance of the medium occurs due to the peculiarities of the internal structure. Direct numerical simulation for a detailed picture of the flow, reflecting the vortices in each pore, was carried out using a grid of 40 million cells. Figure 2 shows the grid quality.



**Figure 2.** Fragment of the grid partitioning of the computational domain.

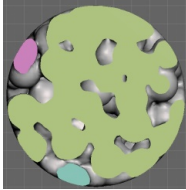
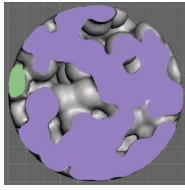
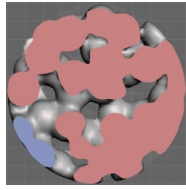
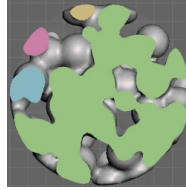
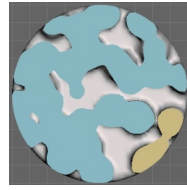
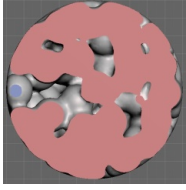
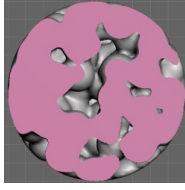
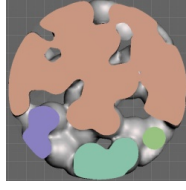
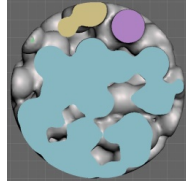

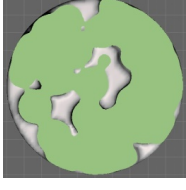
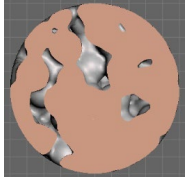
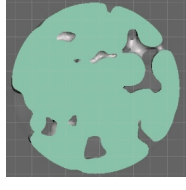
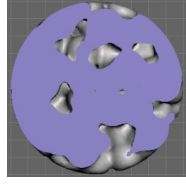
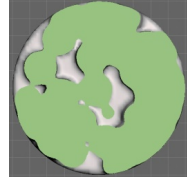
We set the condition "mass flow inlet" at the left border of the computational area corresponding to the flow inlet, and the condition "pressure outlet" at the right border. Also, the remaining boundaries were defined as "wall" automatically. We performed calculations for three values of medium porosity  $\varepsilon = 0.6$ ,  $\varepsilon = 0.7$  and  $\varepsilon = 0.8$ .

### **3. Determination of the parameter $Po$ (porosity)**

We selected five cross sections of the porous layer: 0 cm, 1 cm, 2 cm, 3 cm, and 4 cm from the beginning of the porous section (Table 1) to determine the parameter (counting the average number of pores per inch). The cross-section pictures of the porous medium make it possible to determine the average porosity parameter.

For medium porosity  $\varepsilon = 0.6$ ,  $\varepsilon = 0.7$ ,  $\varepsilon = 0.8$  porosity parameters are  $Po = 6$ ,  $Po = 7$ ,  $Po = 8$  respectively.

**Table1.** Pictures of the cross-section of the open cell foam model.

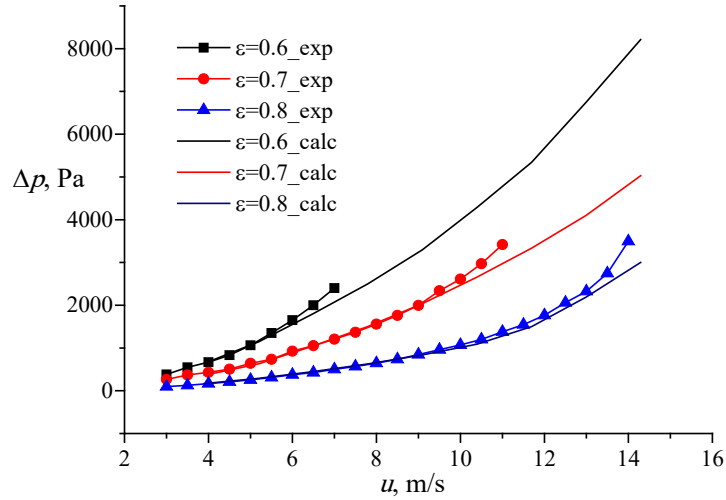
	$l_1 = 0$ cm	$l_2 = 1$ cm	$l_3 = 2$ cm	$l_4 = 3$ cm	$l_5 = 4$ cm
$\varepsilon = 0.6$					
$\varepsilon = 0.7$					
$\varepsilon = 0.8$					

#### 4. Results of experiment and numerical simulation

It is necessary to make sure that the model is correct in order to accurate calculation of the particle deposition efficiency. Experimental samples completely represent the computational model geometry taking into account the inverse structure (the numerical calculation is in the inner porous space). In the experiment, air is injected into the porous medium by a compressor, and the pressure drop is measured by «Testo 510 manometer», the flow rate is measured by «Testo 450 hot-wire anemometer». The pressure drop values in the porous region are determined depending on the average filtration rate. The results of experimental studies and numerical simulations correlate well. The insignificant difference in the study results at high flow velocities is related to developed turbulent flow and difficulty in «trapping» vortices in numerical calculation. It is possible that the grid partition of 40 million cells is not enough for such a complex area, but computational capabilities limit the increase of the grid elements number. The average filtration rate of gas suspension in technical devices varies from 1 to 5 m/s, the deviation in the results of numerical and experimental studies can be acceptable, and at speeds up to 5 m/s, there is a complete agreement of the obtained data.

The particle deposition efficiency is the primary parameter in a filter quality. Also, it is a ratio of the settled particles number to the started particles number:

$$E = \frac{N}{N_0}.$$



**Figure 3.** The pressure drop dependence on the flow rate for three values of the medium porosity: lines with symbols – experimental data, lines without symbols – calculation results.

Helmann [1] derived a semi-empirical dependence for evaluating of the particle deposition efficiency of in diffusion neglect.

$$E = 1 - P, \quad \ln(P) = -\frac{t}{d_f} \cdot (5.486 \cdot St^{2.382} + 3.891 \cdot N_G^{0.88})$$

where  $t$  is the filter thickness,  $d_f$  is the fiber diameter of the porous medium,  $St$  is Stokes number,  $N_G$  is the parameter of gravitational settling.

$$St = \frac{\rho_p \cdot d_p^2 \cdot u_0}{18 \cdot \mu \cdot d_f}, \quad N_G = \frac{\rho_p \cdot d_p^2 \cdot g}{18 \cdot \mu \cdot u_0}$$

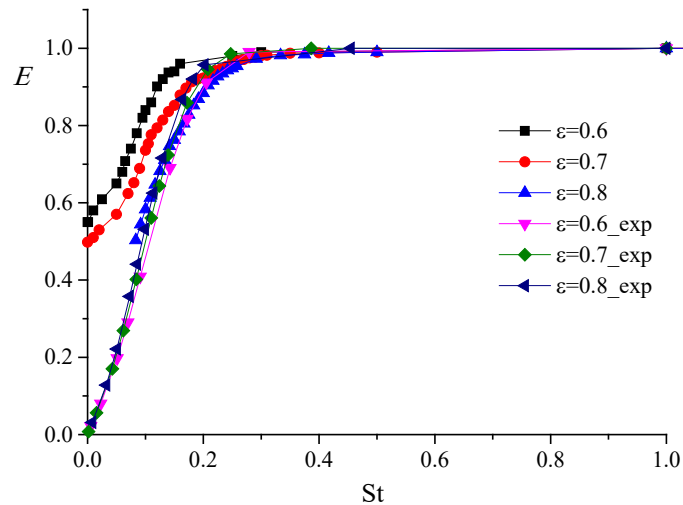
$d_p$  is the particle diameter,  $u_0$  is the gas velocity,  $\mu$  is viscosity.

$$d_f = 0.009633 \cdot Po^{-1.216}$$

The parameters  $t$  and  $d_f$  are given in millimeters.

The correctness confirmation of the model made it possible to calculate the particle deposition efficiency in the gas flow velocity

According to the numerical calculation and the semi-empirical Hellman formula, the efficiency curves of particle deposition correlate well for the case of maximum porosity  $\varepsilon = 0.8$ , however, the efficiency curves diverge for the case of lower porosity because the Hellman formula works only in a certain range of environmental parameters in the performed experiment. The starting particles location is also significant. For a medium with lower porosity, a substantial area is formed in the cross-section, comparable to the pore area on which particles additionally deposited if particles start far from the pores of the filtering material. These two factors explain the discrepancy between the experimental data and the numerical calculation results for the values of medium porosity  $\varepsilon = 0.6$  and  $\varepsilon = 0.7$ .



**Figure 4.** The dependence of the particle deposition efficiency on the Stokes number, obtained by numerical calculations and experimental studies.

## 5. Conclusion

In this work, we investigate the dependence of the medium porosity, which uses the mechanics of porous media and the porosity parameter  $Po$  used in industry. We carried out numerical calculations and experimental studies of the gas flow in a tube containing a porous layer, which is a filter model for various porosities of the medium. The curves of numerical calculation results for the pressure drop values correlate well with the curves of experimental data. The particle deposition efficiency was calculated depending on the Stokes number, we found that the calculations results and experimental data from other authors are entirely consistent for the porosity  $\varepsilon = 0.8$ , and there is a significant difference for  $\varepsilon = 0.7$  and  $\varepsilon = 0.6$  due to the limits of applicability of the semi-empirical formula and the particle start position.

## Acknowledgements

The reported research was funded by Russian Foundation for Basic Research, grant № 19-07-01188.

## References

- [1] Hellmann A, Pitz M, Schmidt K, Haller F and Ripperger S 2015 *Aerosol Sci. Technol.* **49** 16
- [2] Calmidi V V and Mahajan R L 1999 *J. Heat Trans.* **121** (2) 466
- [3] Zhao C Y 2012 *Int. J. Heat Mass Trans.* **55** (13-14) 3618
- [4] Muley A, Kiser C, Sundén B and Shah R K 2012 *Heat Trans. Eng.* **33** (1) 42
- [5] Han X H, Wang Q, Park Y G, T'joen C, Sommers A and Jacobi A 2012 *Heat Trans. Eng.* **33** (12) 991
- [6] Mahjoob S and Vafai K 2008 *Int. J. Heat Mass Trans.* **51** (15-16) 3701
- [7] Nawaz K 2014 *Aerogel coated metal foams for dehumidification applications* (Ph.D., University of Illinois at Urbana-Champaign)
- [8] Dai Z, Nawaz K, Park Y, Chen Q and Jacobi A M 2012 *Heat Trans. Eng.* **33** (1) 21
- [9] Ejlali A, Ejlali A, Hooman K and Gurgenci H 2009 *Int. Com. Heat Mass Trans.* **36** (7) 674
- [10] Boomsma K, Poulikakos D and Zwick F 2003 *Mech. Materials.* **35** (12) 1161
- [11] Baillis D, Raynaud M and Sacadura J F 1999 *J. Thermophys. Heat Trans.* **13** (3) 292
- [12] Lee S C and Cunnington G R 2000 *J. Thermophys. Heat Trans.* **14** (2) 121
- [13] Hayes A M, Khan J A, Shaaban A H and Spearing I G 2008 *Int. J. Thermal Sci.* **47** (10) 1306
- [14] Pavel B I and Mohamad A A 2004 *Int. J. Heat Mass Trans.* **47** (23) 4939

- [15] Al-Raoush R and Alsaleh M 2007 *Powder Technol.* **176** (1) 47
- [16] Beugre D, Calvo S, Dethier G, Crine M, Toye D and Marchot P 2010 *J. Comp. App. Math.* **234** (7) 2128
- [17] Peng Y and Richardson J T 2004 *App. Cat. A: Gen.* **266** (2) 235
- [18] Mardanov R F, Soloveva O V and Zaripov S K 2016 *IOP Conf. Ser.: Materials Sci. Eng.* **158** 012065
- [19] Soloveva O V, Solovev S A, Khusainov R R, Popkova O S and Panenko D O 2018 *J. Phys.: Conf. Ser.* **944** (1) 012113
- [20] Soloveva O V, Solovev S A, Khusainov R R and Shubina A S 2019 *J. Phys.: Conf. Ser.* **1158** (4) 042023
- [21] Solovev S A, Soloveva O V and Popkova O S 2018 *Rus. J. Phys. Chem. A.* **92** (3) 603
- [22] Perrot C, Panneton R and Olny X 2007 *J. App. Phys.* **101** (11) 113538
- [23] Sullivan R M, Ghosn L J and Lerch B A 2008 *Int. J. Solids Structures.* **45** (6) 1754
- [24] Bai M and Chung J N 2011 *Int. J. Therm. Sci.* **50** (6) 869
- [25] Edouard D, Lacroix M, Huu C P and Luck F 2008 *Chem. Eng. J.* **144** (2) 299
- [26] Dietrich B 2012 *Chem. Eng. Sci.* **74** 192
- [27] Mahjoob S and Vafai K 2008 *Int. J. Heat Mass Trans.* **51** (15-16) 3701
- [28] Fourie J G and Du J P 2002 *Chem. Eng. Sci.* **57** (14) 2781
- [29] Bhattacharya A, Calmidi V V and Mahajan R L 2002 *Int. J. Heat Mass Trans.* **45** (5) 1017
- [30] Huu T T, Lacroix M, Huu C P, Schweich D and Edouard D 2009 *Chem. Eng. Sci.* **64** (24) 5131
- [31] Dai Z, Nawaz K, Park Y, Chen Q and Jacobi A M 2012 *Heat Trans. Eng.* **33** (1) 21
- [32] Dukhan N and Chen K C 2007 *Exp. Therm. Fluid Sci.* **32** (2) 624
- [33] Kamath P M, Balaji C and Venkateshan S P 2013 *Int. J. Therm. Sci.* **64** 1
- [34] Chiappini D, Bella G, Festuccia A and Simoncini A 2015 *Com. Comp. Phys.* **18** (3) 707